Biogeosciences Discuss., 11, 7389–7412, 2014
www.biogeosciences-discuss.net/11/7389/2014/
doi:10.5194/bgd-11-7389-2014

Biogeosciences Discussions
Open Access

Diagnosing CO_2 fluxes in the upwelling system off the Oregon coast

Z. Cao[1,*], M. Dai[1], W. Evans[2,3], J. Gan[4], and R. Feely[2]

[1]State Key Laboratory of Marine Environmental Science, Xiamen University, Xiamen, China
[2]Pacific Marine Environmental Laboratory, National Oceanic and Atmospheric Administration, Seattle, Washington, USA
[3]Ocean Acidification Research Center, School of Fisheries and Ocean Sciences, University of Alaska Fairbanks, Fairbanks, Alaska, USA
[4]Division of Environment and Department of Mathematics, Hong Kong University of Science and Technology, Kowloon, Hong Kong, China
[*]now at: GEOMAR/Helmholtz Center for Ocean Research Kiel, Kiel, Germany

Received: 8 March 2014 – Accepted: 30 April 2014 – Published: 21 May 2014

Correspondence to: M. Dai (mdai@xmu.edu.cn)

Published by Copernicus Publications on behalf of the European Geosciences Union.

Abstract

It is generally known that the interplay between the carbon and nutrients supplied from subsurface waters via biological metabolism would determine the CO_2 fluxes in upwelling systems. However, quantificational assessment of such interplay is difficult because of the dynamic nature of both upwelling circulation and the associated biogeochemistry. In this study, the diagnosis approach based upon the carbon/nutrient mass balance in the Ocean-dominated Margin (OceMar) framework was applied to resolve the CO_2 fluxes in the well-known upwelling system in the US west coast off Oregon, using the data collected along two cross-shelf transects from the inner shelf to the open basin in spring/early summer 2007. Through examining the biological consumption on top of the water mass mixing built upon the total alkalinity–salinity relationship, we successfully predicted and semi-analytically resolved the CO_2 fluxes showing strong uptakes from the atmosphere beyond the nearshore regions, primarily resulting from the higher utilization of nutrients relative to dissolved inorganic carbon (DIC) based on their concurrent inputs from the depth. On the other hand, we showed significant CO_2 outgassing in the nearshore regions associated with intensified upwelling and minor biological consumption, where CO_2 fluxes could be simplified without considering DIC/nutrient consumption. We reasoned that our approach in conceptualizing OceMar would be in a steady state with balanced DIC and nutrients via both physical transport and biological alterations in comparable timescales.

1 Introduction

The contemporary coastal ocean, characterized by high primary productivity due primarily to the abundant nutrient inputs from both river plume and coastal upwelling, is generally seen as a significant CO_2 sink at the global scale (Borges et al., 2005; Cai et al., 2006; Chen and Borges, 2009; Laruelle et al., 2010; Borges, 2011; Cai, 2011; Dai et al., 2013). However, mechanistic understanding of the coastal ocean carbon

BGD
11, 7389–7412, 2014

cycle remains limited, leading to the unanswered question of why some coastal systems are sources while others are sinks of atmospheric CO_2. In shaping the concept of the coastal ocean carbon study, we recently proposed a new framework, the Ocean-dominated Margin (OceMar), for mechanistically understanding the CO_2 source/sink nature of an ocean margin (Dai et al., 2013). This framework highlights the importance of the boundary process between the open ocean and the ocean margin, and proposes a semi-analytical diagnosis approach to resolve sea–air CO_2 fluxes. The approach invokes an establishment of the water mass mixing scheme in order to define the physical transport, or the conservative portion of carbon and nutrients from the adjacent open ocean; and the constraint of the biogeochemical alteration of these non-local inputs in the upper waters of ocean margins. The water mass mixing scheme is typically revealed using conservative chemical tracers such as total alkalinity (TAlk) and/or dissolved calcium ion (Ca^{2+}) to bypass identifications of end-members associated with individual water masses that often possess high complexity in any given oceanic regime. The constraint of the biogeochemical alteration can then be estimated as the difference between the predicted values based on conservative mixing between end-members and the field measured values. The relative consumption between dissolved inorganic carbon (DIC) and nutrients determines if DIC is in excess or in deficit relative to the off-site input. Such excess DIC will eventually be released to the atmosphere through air–sea CO_2 exchange. Using two large marginal seas, the South China Sea (SCS) and the Caribbean Sea (CS) as cases, we have successfully predicted, via evaluating DIC and nutrient mass balance, the CO_2 outgassing that is consistent with the field observations (Dai et al., 2013). However, the OceMar concept and the diagnosis approach have not been attested to upwelling systems that can be either sources (e.g., Friederich et al., 2002; Torres et al., 2003; Fransson et al., 2006) or sinks (e.g., Borges et al., 2002; Santana-Casiano et al., 2009; Evans et al., 2012) of atmospheric CO_2. While it is generally known that the interplay between the nutrients and DIC supplied from subsurface waters via biological metabolism would determine the CO_2 fluxes in upwelling systems, quantificational assessment of such interplay is

BGD
11, 7389–7412, 2014

difficult because of the dynamic nature of both upwelling circulation and the associated biogeochemistry.

This study thus chose the well-known upwelling system in the US west coast off Oregon, to examine the CO_2 flux dynamics through our proposed mass balance approach associated with carbon/nutrient coupling. The system under study is featured by a relatively narrow shelf at the northern and southern portions and a direct link with the eastern North Pacific (eNP) offshore (Fig. 1). While strong equatorward winds in spring/summer drive offshore Ekman transport at the surface along the coastline, the carbon and nutrient-rich deep water is transported shoreward and upward over the shelf to compensate for the offshore transport in the surface layer (Allen et al., 1995; Federiuk and Allen, 1995). Outcrops of waters from the depth of 150–200 m are frequently observed in the nearshore on the Oregon shelf, where the surface partial pressure of CO_2 (pCO_2) can reach levels near 1000 µatm. This water is then transported offshore and along shore while the pCO_2 is drawn down by biological productivity to levels of ~ 200 µatm, far below the atmospheric pCO_2 value (Hales et al., 2005, 2012; Feely et al., 2008; Evans et al., 2011). Such a dramatic decrease in seawater pCO_2 might be due to the fact that the complete utilization of the preformed nutrients in the upwelled waters exceeds their corresponding net DIC consumption, leading to the area off Oregon acting as a net sink of atmospheric CO_2 during the upwelling season (Hales et al., 2005). On the other hand, Evans et al. (2011) suggest that the spring/early summer undersaturated pCO_2 conditions in some offshore areas result from nonlocal productivity associated with the Columbia River (CR) plume, which transports ~ 77 % of the total runoff from the western North America to the Pacific Ocean (Hickey, 1989).

In this context, the Oregon shelf in the upwelling season can be a potential OceMar-type system with the majority of DIC and nutrients in the upper layer originating from nonlocal deep waters of the eNP, though riverine inputs might complicate the application of the OceMar framework. On the other hand, upper waters in offshore areas beyond the upwelling circulation on the Oregon shelf would be largely fed by on-site

BGD
11, 7389–7412, 2014

deep waters via diapycnal mixing such as vertical diffusion, with minor influence of the CR plume depending on the circulation and discharges.

2 Study area and data source

2.1 California Current system and upwelling circulation

The upwelling circulation off Oregon is linked with the eastern boundary current, the California Current (CC) occupying the open basin of the eNP (Barth et al., 2000). The CC is a board and weak surface current (0–300 m) which carries low-salinity/temperature water equatorward from the subarctic Pacific. The deeper-lying California Undercurrent (200–500 m), which has relatively high salinity and temperature, originates in the eastern Equatorial Pacific and flows poleward inshore along the west coast of North America (Lynn and Simpson, 1987). The CC system is characterized by coastal upwelling in spring/summer, during which waters primarily composed of the CC is transported upward from the depth of 150–200 m towards the nearshore surface (Castro et al., 2001).

Both field observations and modeling studies (Spitz et al., 2005, and references therein) show that the upwelling circulation pattern over the Oregon shelf differs significantly between north and south of Newport (Fig. 1). North of Newport between 45.0° N and 45.5° N with a relatively straight coastline and narrow shelf, the uniform bottom topography generally results in the typical upwelling situation with a southward coastal jet close to shore at Cascade Head (Fig. 1). Over the central Oregon shelf between 43.5° N and 45.0° N, the highly variable bottom topography over Heceta Bank (Fig. 1) largely influences the upwelling circulation, leading to a complex three-dimensional flow pattern with offshore shifting of the coastal jet and development of northward flow inshore. Along the southern part of the Oregon coast between 42.0° N and 43.0° N, an enhancement of upwelling, jet separation and eddy formation are observed to be as-

BGD
11, 7389–7412, 2014

sociated with interactions of the wind-forced coastal currents with Cape Blanco (Fig. 1) (Gan and Allen, 2005, and references therein).

2.2 Data source

Our data sets were based on the online published carbonate system and nutrient data collected along two transects off Oregon during the first North American Carbon Program (NACP) West Coast Cruise in spring/early summer 2007 (http://cdiac.ornl.gov/oceans/Coastal/NACP_West.html; Feely et al., 2008; Feely and Sabine, 2011). Transect 4 (stations 25–33 from nearshore to offshore) is located off Newport, Oregon, while Transect 5 (station 41–35 from nearshore to offshore) is located off Crescent City near the Oregon–California border. The most offshore stations on both transects were located in the open basin of the eNP (Fig. 1).

3 Results and discussion

The region under study is highly dynamic potentially involving coastal upwelling, the CR plume and the pelagic waters mixed by various Pacific water masses (Hill and Wheeler, 2002). Instead of accounting all of the water masses contributing to the CC system, the mixing scheme in the upper waters along both transects was examined via the total alkalinity–salinity (TAlk–Sal) relationship obtained during the sampling period such as to make quantification of the conservative portion of carbon and nutrients possible. The end-members were therefore defined under this relationship, which might have experienced physical or biological alterations from their original water masses such as the CR and the CC. Subsequently, the biologically consumed DIC and nutrients were quantified as the difference between their conservative values predicted from the derived end-member mixing and the corresponding field measurements. Finally, the CO_2 source/sink nature in the upper waters off Oregon was diagnosed via a mass

BGD
11, 7389–7412, 2014

balance approach by estimating the relative consumption between DIC and nutrients according to Dai et al. (2013).

3.1 Various mixing schemes in the upper 200 m waters off Oregon

In the upper 200 m waters with salinity lower than ~ 34.0, the TAlk–Sal relationship displayed two general phases along Transect 4. One was the linear regression for waters with salinity lower than ~ 32.0 (corresponding to the depth of ~ 10–20 m), having an intercept of ~ 1200 µmol kg^{-1}. This value agreed well with the observed TAlk of ~ 1000 µmol kg^{-1} in the main stream of the CR (Park et al., 1969b; Evans et al., 2013). The other was the linear regression for waters with salinity between ~ 32.0 and ~ 34.0 (corresponding to the depth of ~ 200 m), where the smaller intercept of ~ 500 µmol kg^{-1} implied a smaller contribution from the CR plume (Fig. 2a). Exceptions were observed at the shallowest station 25 (water depth ~ 50 m) and the deepest station 33 (water depth ~ 2900 m). The TAlk–Sal relationship completely followed the second phase for the upper 200 m waters at station 33 (Fig. 2a), suggesting a small fraction of the CR plume even in the surface waters of this outmost station on Transect 4. On the other hand, data points of the two parameters were not well correlated through the entire water column of station 25 and fell off either regression line (Fig. 2a). The water mass mixing at this innermost station was not as straightforward, despite minor freshwater admixture as suggested by the high surface salinity of > 32.0.

In contrast, all salinity values, including surface samples in the upper 200 m waters on Transect 5, were higher than 32.0 (Fig. 2b). The TAlk–Sal relationship also displayed two phases. One was the linear regression for stations 35–38 deeper than ~ 800 m, with slope and intercept values comparable to the second phase observed on Transect 4. The other was the linear regression for the three shallow stations largely influenced by coastal upwelling (Feely et al., 2008) (Fig. 2b). The salinity in the upper 200 m waters at station 39 and in the entire water column of stations 40 and 41 varied within a much smaller range, with insignificant freshwater input with zero solutes as indicated by the negligible intercept of the TAlk–Sal regression (Fig. 2b).

BGD
11, 7389–7412, 2014

All phases shown in Fig. 2 displayed very good linear TAlk–Sal relationships, indicating an overall two end-member mixing scheme for each phase. However, such two end-member mixing was not spatially homogeneous in the upper waters off Oregon during the sampling period. The top waters at stations 26–32 on Transect 4 were imprinted by the CR plume with salinity around ~ 30.0. During the transport from the mouth of the CR estuary, the plume water increasingly mixed with adjacent oceanic waters, largely feeding its pathway. However, the majority of DIC and nutrients in waters immediately below the buoyant layer, as well as in surface waters at station 33 and possibly at station 25, should originate from deep waters through coastal upwelling and/or vertical mixing. The influence of the CR plume still occurred but was diluted by other freshwater masses such as rainwater, suggesting a mixing scheme between the deep water of the eNP and a combined freshwater end-member (Park, 1966, 1968). Such mixing was also applicable to the surface waters at stations 35–38 on Transect 5. On the other hand, the upper 200 m waters or the entire water column at stations 39–41 on Transect 5 should result from a simple two end-member mixing between the upwelling source water in the CC and the rainwater with zero solutes, establishing for them an apparent OceMar-type system.

3.2 ΔDIC and Δ NO_3 in the upper waters off Oregon

The defined mixing schemes enabled us to estimate the nonconservative portion of DIC (ΔDIC) and nitrate (ΔNO_3) in the upper waters off Oregon following Dai et al. (2013):

$$\Delta DIC = DIC^{cons} - DIC^{meas} \quad (1)$$

$$\Delta NO_3 = NO_3{}^{cons} - NO_3{}^{meas} \quad (2)$$

$$X^{cons} = \frac{Sal^{meas}}{Sal^{ref}} \times (X^{ref} - X^{eff}) + X^{eff} \quad (3)$$

The superscripts “cons” and “meas” in Eqs. (1) and (2) denote conservative-mixing induced and field measured values. In Eq. (3), X represents DIC or NO_3 while Sal^{meas}

BGD
11, 7389–7412, 2014

is the CTD measured salinity. Sal^{ref} and X^{ref} are the reference salinity and concentration of DIC or NO_3 for the deep water end-member, which are the averages of all ~ 200 m samples from stations involved in each mixing scheme. Specifically, for waters immediately below the top buoyant layer at stations 27–32 and waters in the surface mixed layer at stations 25 and 33 on Transect 4, the deep water end-member values of the reference salinity and concentrations of DIC or NO_3 were the averages of ~ 200 m samples from stations 28–33 (Fig. 1). On Transect 5, the preformed salinity, DIC and NO_3 values for waters in the surface mixed layer at stations 35–38 were the averages of ~ 200 m samples of these stations. For the upper waters at stations 39–41 influenced by the intensified upwelling, the deep water end-member was selected as the ~ 200 m water at station 39 (Fig. 1).

The X^{eff} in Eq. (3) denotes the effective concentration of DIC or NO_3 sourced from the freshwater input to various zones off Oregon. Since rainwater was assumed to have no solute, both DIC^{eff} and $NO_3{}^{eff}$ would be zero for waters in the surface mixed layer of stations 39–41 on Transect 5. On the other hand, the estimation of X^{eff} associated with the CR followed the method for the OceMar case study of the CS, which has a noticeable DIC^{eff} from the combination of the Amazon River and the Orinoco River (Dai et al., 2013).

Since bicarbonate dominates other CO_2 species and other alkalinity components, DIC concentrations in the main stream of the CR are numerically similar to TAlk, which are also around ~ 1000 µmol kg^{-1} (Park et al., 1969a, 1970). This value was taken as the DIC end-member of the CR. The NO_3 end-member value was selected as 15 µmol kg^{-1} based on recent years' observations in May and July at station SATURN-05 established in the upstream CR (database of the Center for Coastal Margin Observation and Prediction; http://www.stccmop.org/datamart/observation_network/fixedstation?id=saturn05#anchor_5). Assuming that the biological consumption of DIC and NO_3 in the CR plume followed the Redfield ratio (Redfield et al., 1963), the DIC removal was estimated to be

BGD
11, 7389–7412, 2014

$\sim 100\,\mu mol\,kg^{-1}$ (approximately $15 \cdot 106/16$), while NO_3 was rapidly consumed along the pathway of the CR plume and generally depleted in the area beyond the plume (Aguilar-Islas and Bruland, 2006; Lohan and Bruland, 2006). As a consequence, the complete DIC^{eff} and NO_3^{eff} in the upper waters off Oregon from the CR would be $\sim 900\,\mu mol\,kg^{-1}$ and $\sim 0\,\mu mol\,kg^{-1}$.

If the combined freshwater end-member was a mixture of the CR and the rainwater with zero solutes, the intercept values of 517.5±29.2 (Fig. 2a) and 677.4±32.2 (Fig. 2b) derived from the TAlk–Sal regression indicated that the CR fractions were ~ 50 % and ~ 65 % (approximately 500/1000 and 650/1000 by taking $\sim 1000\,\mu mol\,kg^{-1}$ as the TAlk end-member value of the CR, Park et al., 1969b; Evans et al., 2013). The DIC^{eff} from the freshwater input was thus estimated to be $\sim 450\,\mu mol\,kg^{-1}$ (approximately $900 \cdot 50$ %) for waters immediately below the top buoyant layer at stations 27–32 and waters in the surface mixed layer at stations 25 and 33 on Transect 4, which was slightly lower than that of $\sim 585\,\mu mol\,kg^{-1}$ (approximately $900 \cdot 65$ %) for waters in the surface mixed layer at stations 35–38 on Transect 5. The NO_3^{eff} in any combined freshwater end-member was zero.

Note that numerous small rivers are distributed on the Oregon Coast, which might also have diluted the CR plume inducing the lower intercept of the TAlk–Sal regression observed on Transects 4 and 5 (Fig. 2). The average wintertime discharge from these Coast Range rivers is estimated to be $\sim 2570\,m^3\,s^{-1}$ (Wetz et al., 2006), which is more than an order of magnitude higher than that in the summer (Colbert and McManus, 2003; Sigleo and Frick, 2003). However, the CR discharge in May to June 2007 reached its summit of $\sim 15\,000\,m^3\,s^{-1}$ (Evans et al., 2013), which should be approximately two orders of magnitude higher than the discharge of small rivers. This significant contrast would suggest that inputs from small rivers should be negligible compared to the CR plume. In particular, inputs from small rivers are normally restricted to a narrow band near the coast, whereas the research domain of this study has extended to the open basin of the eNP. Even the surface salinity at the innermost stations (i.e., station 25

BGD
11, 7389–7412, 2014

on Transect 4 and station 41 on Transect 5; Fig. 1) was as high as ~ 32.5 and ~ 34.0, respectively, which would rule out the influence of small rivers.

3.3 Evaluating the CO_2 source/sink nature in the upper waters off Oregon

The coupling of DIC and NO_3 dynamics could be then examined based on the classic Redfield ratio of C : N = 106 : 16 = 6.6 (Redfield et al., 1963). Positive values of the difference between ΔDIC and 6.6ΔNO_3 (ΔDIC–6.6ΔNO_3) suggested a CO_2 source term since "excess ΔDIC" was removed by CO_2 degassing into the atmosphere. In contrast, negative ΔDIC–6.6ΔNO_3 suggested that "deficient ΔDIC" was supplied via the atmospheric CO_2 input to the ocean representing a CO_2 sink. Such net CO_2 exchange between the seawater and the atmosphere was further quantified as the sea–air difference of pCO_2 (ΔpCO_2) via the Revelle factor (RF), which is referred to as the fractional change in seawater CO_2 over that of DIC at a given temperature, salinity and alkalinity and indicates the ocean's sensitivity to an increase in atmospheric CO_2 (Revelle and Suess, 1957; Sundquist et al., 1979). Because pCO_2 and CO_2 are proportional to each other, the RF can be illustrated as

$$\mathrm{RF} = \frac{\partial pCO_2 / pCO_2}{\partial \mathrm{DIC} / \mathrm{DIC}} \tag{4}$$

The sea–air ΔpCO_2 (i.e., ∂pCO_2) is thus obtained by

$$\text{Sea–air } \Delta pCO_2 = \mathrm{RF} \times pCO_2 \times \frac{\partial \mathrm{DIC}}{\mathrm{DIC}} \tag{5}$$

Here pCO_2 and DIC are the atmospheric pCO_2 (given an initial balance of sea–air CO_2 exchange) and sea surface DIC, respectively, and ∂DIC equals ΔDIC–6.6ΔNO_3.

As shown in Fig. 3, the estimated ΔDIC–6.6ΔNO_3 values and their corresponding sea–air ΔpCO_2 in the upper waters off Oregon were overall below zero, suggesting a significant CO_2 sink nature.

BGD
11, 7389–7412, 2014

3.3.1 Transect 4

On Transect 4 off Newport, the average value of $\Delta DIC–6.6\Delta NO_3$ was $-23 \pm 2\ \mu mol\ kg^{-1}$ in waters immediately below the top buoyant layer at stations 27–32, which equaled the average value for the surface mixed layer at station 33 (Fig. 3a). Although located at different depths, the two water parcels experienced similar physical mixing and biogeochemical modifications inducing the same CO_2 signature. The former water mass should work as a CO_2 sink when in contact with the atmosphere before or after the passage of the episodic CR plume. The average sea–air ΔpCO_2 resulting from the combined deficient ΔDIC was $-54 \pm 4\ \mu atm$ (Fig. 3a). Given the atmospheric pCO_2 of $\sim 390\ \mu atm$ (Evans et al., 2011), the seawater pCO_2 in these regions was thus estimated to be $336 \pm 4\ \mu atm$, which agreed rather well with the field measurements of $334 \pm 13\ \mu atm$ (the underway seawater pCO_2 data were not available online but alternatively calculated by applying TAlk and DIC data into the CO2SYS program, Lewis and Wallace, 1998).

The diagnosis approach was not applied to the top buoyant layer since the aged CR plume might have experienced complex mixing with various surrounding water masses during its transport, as indicated by the scatter TAlk–Sal relationship (Fig. 2a). However, the far-field CR plume is suggested to be a strong sink of atmospheric CO_2 due to earlier biological consumption (Evans et al., 2011), which was supported by the observed low pCO_2 of $\sim$ 220–300 µatm in the top buoyant layer on Transect 4. As a consequence, the CO_2 sink nature in the upper waters from the outer shelf (bottom depth of station 27 was ~ 170 m) to the open basin off Newport, Oregon would primarily result from the higher utilization of nutrients relative to DIC based on their concurrent inputs from deep waters. The nonlocal high productivity in the CR plume could inject even lower pCO_2 but this effect would be transitory.

At the innermost station 25 on Transect 4, highly positive values of $\Delta DIC–6.6\Delta NO_3$ and sea–air ΔpCO_2 were obtained for the surface mixed layer of this station, indicating a significant CO_2 source. However, the lowest pCO_2 value of $\sim 170\ \mu atm$ was observed

BGD
11, 7389–7412, 2014

in these nearshore waters off Oregon. The poor correlation between TAlk and salinity at station 25 (Fig. 2a) might compromise the estimation, whereas the same method (Eqs. 1–5) was successfully applied to other stations on Transect 4 with a distinct TAlk–Sal relationship (i.e., the second phase in Fig. 2a). Note that coastal upwelling clearly influenced the bottom water at station 25 as indicated by the comparable salinity and TAlk values to those in offshore 200 m waters. Instead of being fed by the upwelled deep water, the DIC and nutrients in the surface mixed layer might have originated from horizontal admixture of the surrounding waters. These waters possibly experienced intense diatom blooms due to the fact that the surface silicate concentrations at station 25 were almost zero, which led to the most undersaturated pCO_2 condition observed in the upper waters off Oregon.

3.3.2 Transect 5

On Transect 5 near the Oregon–California border, the average $\Delta DIC–6.6\Delta NO_3$ and sea–air ΔpCO_2 were estimated to be $-20 \pm 3\,\mu mol\,kg^{-1}$ and $-48 \pm 8\,\mu atm$ in the surface mixed layer of offshore stations 35–38 (Fig. 3b). Both values were comparable to those obtained from Transect 4, indicating a similar magnitude of the CO_2 sink term. The estimated sea surface pCO_2 of $342 \pm 8\,\mu atm$ was consistent with the field measurements of $332 \pm 12\,\mu atm$ in this region.

The $\Delta DIC–6.6\Delta NO_3$ and sea–air ΔpCO_2 in the surface mixed layer of stations 39–41, although still below zero, were obviously higher than those of stations 35–38 (Fig. 3b). Such an increase was expected since stations 39–41 were located in the area with the most intense upwelling, which brought CO_2-rich deep waters to the nearshore surface (Feely et al., 2008). However, our estimation suggested a weaker CO_2 sink or close to being in equilibrium with the estimated sea surface pCO_2 of $367 \pm 12\,\mu atm$, whereas the field measurements of $\sim 650–1000\,\mu atm$ indicated that the coastal upwelling zone should be a very strong source of CO_2 to the atmosphere.

A uniform salinity of ~ 34.0 through the entire water column was observed at stations 40 and 41 due to the outcrop of the upwelling source water at the surface of the inner

BGD
11, 7389–7412, 2014

shelf on Transect 5 (Feely et al., 2008). Although salinity in the surface mixed layer at station 39 was lower, around ~ 33.4, the dilution effect of rainwater should be negligible. After removing the rainwater from the mixing scheme and calculating ΔDIC and ΔNO_3 by directly subtracting the field observed value from the end-member value for the upwelling source water (Eqs. 6 and 7; DIC^{ref} and NO_3^{ref} were field measurements of ~ 200 m water samples at station 39), the ΔDIC–6.6ΔNO_3 values were rapidly increased to above zero in the surface mixed layer at stations 39 and 40, while values at station 41 with a small increase were still overall below zero (Fig. 4a). Correspondingly, the estimated sea surface pCO_2 values were higher than the atmospheric CO_2 value at stations 39 and 40 while they were slightly lower than that at station 41. However, these values still largely fell below the field measurements of seawater pCO_2, displaying shoreward increasing differences from ~ 200 µatm to ~ 700 µatm (Fig. 4b).

$$\Delta DIC = DIC^{ref} - DIC^{meas} \quad (6)$$

$$\Delta NO_3 = NO_3^{ref} - NO_3^{meas} \quad (7)$$

With or without taking rainwater into account, our diagnosis approach did not work in the nearshore with strong upwelling off Oregon, even though the mixing scheme of this region was in accordance with the OceMar concept. We contend that OceMar assumes a steady state with balanced DIC and nutrients via both physical mixing and biological alterations in comparable timescales. However, the continuous inputs from the coastal upwelling might have led to the accumulation of DIC and nutrients in the nearshore surface, which could not be timely consumed by the phytoplankton community, suggesting a possible nonsteady state. Fassbender et al. (2011) estimate that the age of the surface mixed layer at nearshore stations on Transect 5 is only ~ 0.2 days, during which the DIC and NO_3 consumption via organic carbon production was almost zero and $CaCO_3$ dissolution contributed a small fraction to the slightly elevated DIC in the upwelled waters. They further predict that the nearshore surface pCO_2 on Transect 5 would decrease to levels of ~ 200 µatm in ~ 30 days until NO_3 exhaustion via continued biological productivity, implying the achievement of a steady state (Fassbender

BGD
11, 7389–7412, 2014

et al., 2011). Minor biological responses during the intensified upwelling period were also observed in summer 2008, allowing highly oversaturated pCO_2 surface water to persist on the inner shelf off Oregon for even nearly two months (Evans et al., 2011). At this point, it is uncertain why there was such a prolonged delay from the phytoplankton community to the persistent source of upwelled DIC and nutrients. Note that under the condition of more prevailing upwelling-favorable wind as a predicted consequence of climate change (e.g., Snyder et al., 2003; Diffenbaugh et al., 2004), the nearshore off Oregon in the upwelling season might always be in a nonsteady state, since fewer periodic relaxation events or reversals would further decrease the chance for the biological response to be factored in.

In addition, the negligible biological consumption might involve large errors when calculating Δ. The portion of ΔDIC and ΔNO_3 at station 41 relative to the preformed values of the upwelling source water were only ~ 0.5 % and ~ 10 %, slightly higher than the measurement uncertainties. The portion of DIC and NO_3 consumption in the surface mixed layer at offshore stations on Transect 5 were, however, one order of magnitude higher (~ 7 % and ~ 90 %, respectively). This contrast might partially explain why the OceMar framework did not work when insignificant biological alterations occurred. Given the predominant control of physical mixing, we contend that the prediction of the CO_2 flux in the nearshore off Oregon with intensified upwelling could be simplified without considering DIC/nutrient consumption. In other words, surface CO_2 levels in this region were simply imprints of the upwelling source water (pCO_2 ~ 1100 µatm at ~ 150–200 m) with minor dilution by rainwater.

4 Concluding remarks

The semi-analytical diagnosis approach of mass balance that couples physical transport and biogeochemical alterations was well applied to CO_2 sink zones off Oregon extending from the outer shelf to the open basin. In these zones without significant influence of the CR plume, the source of DIC was largely from deep waters of the eNP and

BGD
11, 7389–7412, 2014

the ultimate CO_2 sink nature was determined by the higher nutrient consumption than DIC in the upper waters. On the other hand, the estimated CO_2 flux was opposite to field observations in the coastal upwelling zone along the Oregon coast, which behaved like a typical OceMar system in terms of its mixing process. This discrepancy was very likely due to minor biological responses during the intensified upwelling period, making our mass balance approach based on the coupled physical biogeochemistry invalid. It suggested that the applicability of the proposed semi-analytical diagnosis approach is limited to steady state systems with comparable timescales of water mass mixing and biogeochemical reactions. In such physical mixing prevailing regime, resolving the CO_2 fluxes could be simplified without considering biological consumption of DIC and nutrients. Further work is however needed to understand the carbon and nutrient dynamics as well as the timing between physics and biology associated with coastal upwelling.

Acknowledgements. This work was funded by the National Natural Science Foundation of China through grants 91328202, 41121091, 90711005, and 41130857, and the National Basic Research Program (973) sponsored by the Ministry of Science and Technology through grant 2009CB421200. We are very grateful to the Carbon Dioxide Information Analysis Center (CDIAC; http://cdiac.ornl.gov/oceans/) for the online published data of the first North American Carbon Program (NACP) West Coast Cruise. Zhimian Cao is supported by the Humboldt Research Fellowship for postdoctoral researchers provided by the Alexander von Humboldt Foundation. We thank John Hodgkiss for his help with English.

References

Aguilar-Islas, A. M. and Bruland, K. W.: Dissolved manganese and silicic acid in the Columbia River plume: a major source to the California current and coastal waters off Washington and Oregon, Mar. Chem., 101, 233–247, 2006.

Allen, J. S., Newberger, P. A., and Federiuk, J.: Upwelling circulation on the Oregon continental shelf. Part I: Response to idealized forcing, J. Phys. Oceanogr., 25, 1843–1866, 1995.

BGD
11, 7389–7412, 2014

Barth, J. A., Pierce, S. D., and Smith, R. L.: A separating coastal upwelling jet at Cape Blanco, Oregon and its connection to the California Current System, Deep-Sea Res. Pt. II, 47, 783–810, 2000.

Borges, A. V.: Present day carbon dioxide fluxes in the coastal ocean and possible feedbacks under global change, in: Oceans and the Atmospheric Carbon Content, edited by: Duarte, P. and Santana-Casiano, J. M., Springer Science + Business Media B. V., chap. 3, 47–77, 2011.

Borges, A. V. and Frankignoulle, M.: Distribution of surface carbon dioxide and air–sea exchange in the upwelling system off the Galician coast, Global Biogeochem. Cy., 16, 1020, doi:10.1029/2000GB001385, 2002.

Borges, A. V., Delille, B., and Frankignoulle, M.: Budgeting sinks and sources of CO_2 in the coastal ocean: diversity of ecosystems counts, Geophys. Res. Lett., 32, L14601, doi:10.1029/2005GL023053, 2005.

Cai, W.-J.: Estuarine and coastal ocean carbon paradox: CO_2 sinks or sites of terrestrial carbon incineration?, Annu. Rev. Mar. Sci., 3, 123–145, 2011.

Cai, W.-J., Dai, M., and Wang, Y.: Air–sea exchange of carbon dioxide in ocean margins: a province-based synthesis, Geophys. Res. Lett., 33, L12603, doi:10.1029/2006GL026219, 2006.

Castro, C. G., Chavez, F. P., and Collins, C. A.: Role of the California Undercurrent in the export of denitrified waters from the eastern tropical North Pacific, Global Biogeochem. Cy., 15, 819–830, doi:10.1029/2000GB001324, 2001.

Chase, Z., Strutton, P. G., and Hales, B.: Iron links river runoff and shelf width to phytoplankton biomass along the U.S. West Coast, Geophys. Res. Lett., 34, L04607, doi:10.1029/2006GL028069, 2007.

Chen, C.-T. A. and Borges, A. V.: Reconciling opposing views on carbon cycling in the coastal ocean: continental shelves as sinks and near-shore ecosystems as sources of atmospheric CO_2, Deep-Sea Res. Pt. II, 56, 578–590, 2009.

Colbert, D. and McManus, J.: Nutrient biogeochemistry in an upwelling-influenced estuary of the Pacific Northwest (Tillamook Bay, Oregon, USA), Estuaries, 26, 1205–1219, 2003.

Dai, M., Cao, Z., Guo, X., Zhai, W., Liu, Z., Yin, Z., Xu, Y., Gan, J., Hu, J., and Du, C.: Why are some marginal seas sources of atmospheric CO_2?, Geophys. Res. Lett., 40, 2154–2158, doi:10.1002/grl.50390, 2013.

BGD
11, 7389–7412, 2014

Diffenbaugh, N. S., Snyder, M. A., and Sloan, L. C.: Could CO_2-induced land-cover feedbacks alter near-shore upwelling regimes?, P. Natl. Acad. Sci. USA, 101, 27–32, 2004.
Evans, W., Hales, B., and Strutton, P. G.: Seasonal cycle of surface ocean pCO_2 on the Oregon shelf, J. Geophys. Res., 116, C05012, doi:10.1029/2010JC006625, 2011.
Evans, W., Hales, B., Strutton, P. G., and Ianson, D.: Sea–air CO_2 fluxes in the western Canadian coastal ocean, Prog. Oceanogr., 101, 78–91, 2012.
Evans, W., Hales, B., and Strutton, P. G.: pCO_2 distributions and air–water CO_2 fluxes in the Columbia River estuary, Estuar. Coast. Shelf S., 117, 260–272, 2013.
Fassbender, A. J., Sabine, C. L., Feely, R. A., Langdon, C., and Mordy, C. W.: Inorganic carbon dynamics during northern California coastal upwelling, Cont. Shelf Res., 31, 1180–1192, 2011.
Federiuk, J. and Allen, J. S.: Upwelling circulation on the Oregon continental shelf. Part II: Simulations and comparisons with observations, J. Phys. Oceanogr., 25, 1867–1889, 1995.
Feely, R. and Sabine, C.: Carbon dioxide and hydrographic measurements during the 2007 NACP West Coast Cruise, Carbon Dioxide Information Analysis Center, Oak Ridge National Laboratory, US Department of Energy, Oak Ridge, Tennessee, available at: http://cdiac.ornl.gov/ftp/oceans/NACP_West_Coast_Cruise_2007/, 2011.
Feely, R. A., Sabine, C. L., Hernandez-Ayon, J. M., Ianson, D., and Hales, B.: Evidence for upwelling of corrosive "acidified" water onto the continental shelf, Science, 320, 1490–1492, 2008.
Fransson, A., Chierici, M., and Nojiri, Y.: Increased net CO_2 outgassing in the upwelling region of the southern Bering Sea in a period of variable marine climate between 1995 and 2001, J. Geophys. Res., 111, C08008, doi:10.1029/2004JC002759, 2006.
Friederich, G. E., Walz, P. M., Burczynski, M. G., and Chavez, F. P.: Inorganic carbon in the central California upwelling system during the 1997–1999 El Niño–La Niña event, Prog. Oceanogr., 54, 185–203, 2002.
Gan, J. and Allen, J. S.: Modeling upwelling circulation off the Oregon coast, J. Geophys. Res., 110, C10S07, doi:10.1029/2004JC002692, 2005.
Hales, B., Takahashi, T., and Bandstra, L.: Atmospheric CO_2 uptake by a coastal upwelling system, Global Biogeochem. Cy., 19, GB1009, doi:10.1029/2004GB002295, 2005.
Hales, B., Struttong, P. G., Saraceno, M., Letelier, R., Takahashi, T., Feely, R., Sabine, C., and Chavez, F.: Satellite-based prediction of pCO_2 in coastal waters of the eastern North Pacific, Prog. Oceanogr., 103, 1–15, 2012.

BGD
11, 7389–7412, 2014

Hickey, B. M.: Patterns and processes of circulation over the Washington continental shelf and slope, in: Coastal Oceanography of Washington and Oregon, Elsevier Sci., New York, 41–115, doi:10.1016/S0422-9894(08)70346-5, 1989.

Hill, J. K. and Wheeler, P. A.: Organic carbon and nitrogen in the northern California current system: comparison of offshore, river plume, and coastally upwelled waters, Prog. Oceanogr., 53, 369–387, 2002.

Laruelle, G. G., Dürr, H. H., Slomp, C. P., and Borges, A. V.: Evaluation of sinks and sources of CO_2 in the global coastal ocean using a spatially-explicit typology of estuaries and continental shelves, Geophys. Res. Lett., 37, L15607, doi:10.1029/2010GL043691, 2010.

Lewis, E. and Wallace, D. W. R.: Program Developed for CO_2 System Calculations, ORNL/CDIAC-105, Carbon Dioxide Information Analysis Center, Oak Ridge National Laboratory, US Department of Energy, Oak Ridge, TN, 1998.

Lohan, M. C. and Bruland, K. W.: The importance of vertical mixing for the supply of nitrate and iron to the Columbia River plume: implications for biology, Mar. Chem., 98, 260–273, 2006.

Lynn, R. J. and Simpson, J. J.: The California Current system: the seasonal variability of its physical characteristics, J. Geophys. Res., 92, 12947–12966, 1987.

Park, P. K.: Columbia River plume identification by specific alkalinity, Limnol. Oceanogr., 11, 118–120, 1966.

Park, P. K.: Alkalinity and pH off the coast of Oregon, Deep-Sea Res., 15, 171–183, 1968.

Park, P. K., Gordon, L. I., Hager, S. W., and Cissell, M. C.: Carbon dioxide partial pressure in the Columbia river, Science, 166, 867–868, 1969a.

Park, P. K., Webster, G. R., and Yamamoto, R.: Alkalinity budget of the Columbia River, Limnol. Oceanogr., 14, 559–567, 1969b.

Park, P. K., Catalfomo, M., Webster, G. R., and Reid, B. H.: Nutrients and carbon dioxide in the Columbia river, Limnol. Oceanogr., 15, 70–79, 1970.

Redfield, A. C., Ketchum, B. H., and Richards, F. A.: The influence of organisms on the composition of seawater, in: The Sea, edited by: Hill, M. N., Wiley, New York, 26–77, 1963.

Revelle, R. and Suess, H. E.: Carbon dioxide exchange between atmosphere and ocean and the question of an increase of atmospheric CO_2 during the past decades, Tellus, 9, 18–27, 1957.

Santana-Casiano, J. M., González-Dávila, M., and Ucha, I. R.: Carbon dioxide fluxes in the Benguela upwelling system during winter and spring: a comparison between 2005 and 2006, Deep-Sea Res. Pt. II, 56, 533–541, 2009.

BGD
11, 7389–7412, 2014

Sigleo, A. C. and Frick, W. E.: Seasonal variations in river flow and nutrient concentrations in a northwestern USA watershed, in: First Interagency Conference on Research in the Watersheds, edited by: Renard, K. G., McElroy, S. A., Gburek, W. J., Canfield, H. E., and Scott, R. L., US Department of Agriculture, 370–376, 2003.

Snyder, M. A., Sloan, L. C., Diffenbaugh, N. S., and Bell, J. L.: Future climate change and upwelling in the California Current, Geophys. Res. Lett., 30, 1823, doi:10.1029/2003GL017647, 2003.

Spitz, Y. H., Allen, J. S., and Gan, J.: Modeling of ecosystem processes on the Oregon shelf during the 2001 summer upwelling, J. Geophys. Res., 110, C10S17, doi:10.1029/2005JC002870, 2005.

Sundquist, E. T., Plummer, L. N., and Wigley, T. M. L.: Carbon dioxide in the ocean surface: the homogenous buffer factor, Science, 204, 1203–1205, 1979.

Torres, R., Turner, D. R., Rutllant, J., and Lefèvre, N.: Continued CO_2 outgassing in an upwelling area off northern Chile during the development phase of El Niño 1997–1998 (July 1997), J. Geophys. Res., 108, 3336, doi:10.1029/2000JC000569, 2003.

Wetz, M. S., Hales, B., Chase, Z., Wheeler, P. A., and Whitney, M. M.: Riverine input of macronutrients, iron, and organic matter to the coastal ocean off Oregon, U.S.A., during the winter, Limnol. Oceanogr., 51, 2221–2231, 2006.

BGD
11, 7389–7412, 2014

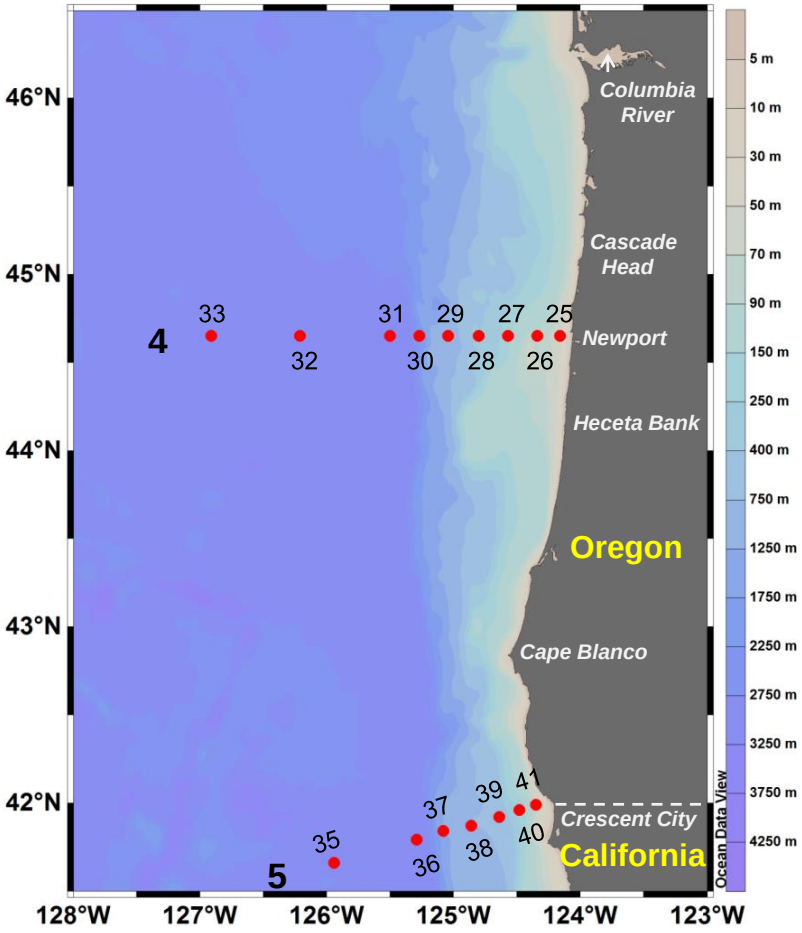

Figure 1. Map of the US west coast off Oregon showing the topography and the locations of sampling stations along Transects 4 and 5 in spring/early summer 2007.

BGD
11, 7389–7412, 2014

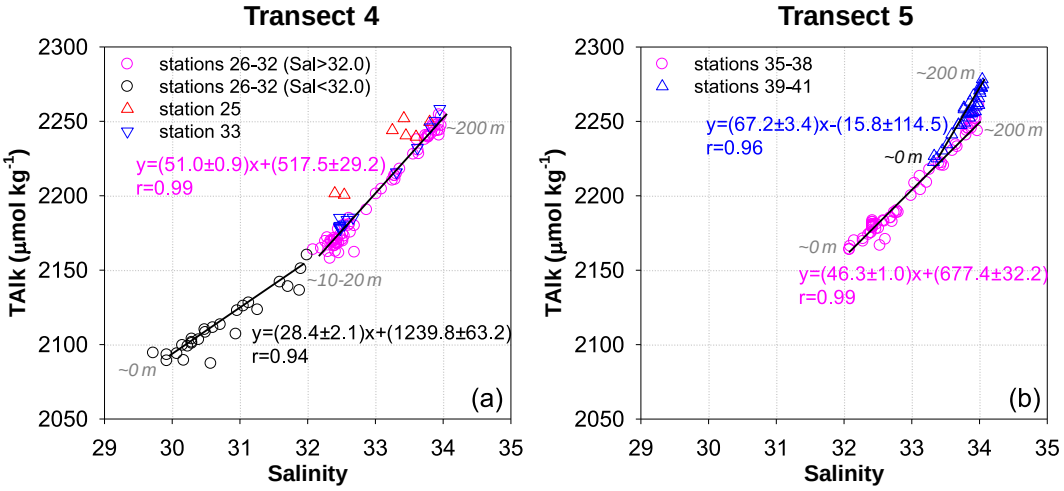

Figure 2. Total alkalinity vs. salinity (TAlk–Sal relationship) in the upper 200 m waters of sampling stations along Transects 4 **(a)** and 5 **(b)** off Oregon in spring/early summer 2007. The solid lines as well as the equations (in accordance with the symbol colors) indicate the linear regression analyses of the TAlk–Sal relationship for various stations. The numbers in italic denote the sampling depth of the endpoints of each line. In **(a)**, the TAlk–Sal relationship at station 26–32 displayed two phases for waters with salinity lower and higher than ~ 32.0. The top waters at these stations were imprinted by the Columbia River plume. In **(b)**, stations 39–41 were largely influenced by coastal upwelling.

BGD
11, 7389–7412, 2014

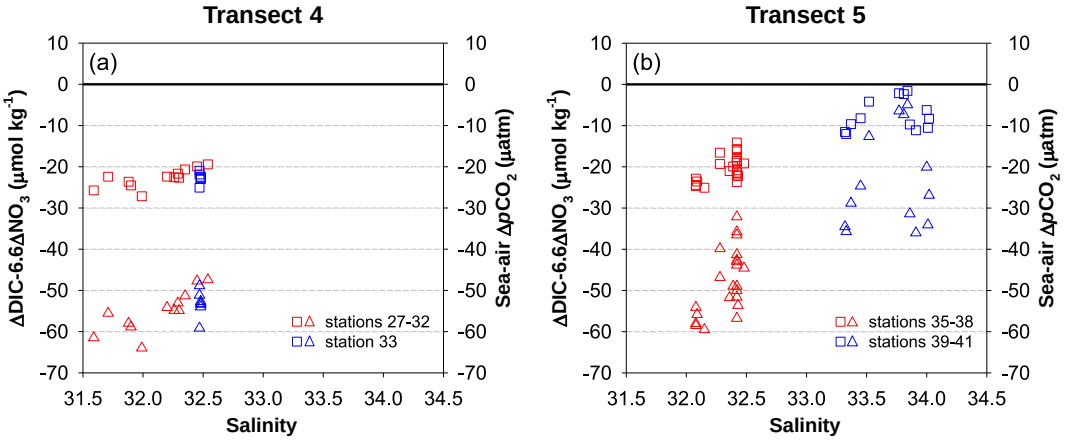

Figure 3. $\Delta DIC–6.6\Delta NO_3$ (squares) and sea–air ΔpCO_2 (triangles) vs. salinity in the upper waters on Transects 4 **(a)** and 5 **(b)** off Oregon in spring/early summer 2007. Note that data for stations 27–32 on Transect 4 were obtained from waters immediately below the top buoyant layer, while data for other stations were obtained from the surface mixed layer. The value of 6.6 is the Redfield C/N uptake ratio (approximately 106/16; Redfield et al., 1963). The solid line indicates the pCO_2 equilibrium between the seawater and the atmosphere.

BGD
11, 7389–7412, 2014

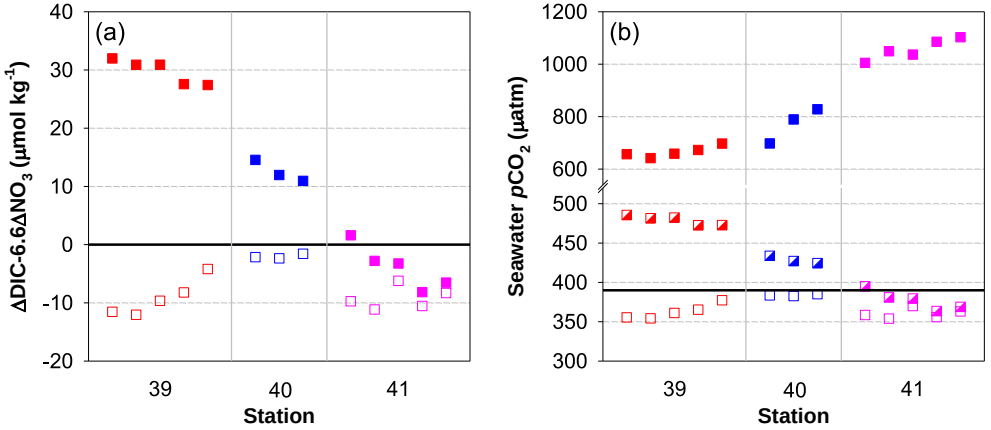

Figure 4. $\Delta DIC–6.6\Delta NO_3$ **(a)** and seawater pCO_2 **(b)** in the surface mixed layer at stations 39–41 on Transect 5 near the Oregon–California border in spring/early summer 2007. In **(a)**, open symbols indicate values estimated based on the two end-member mixing between the upwelling source water and the rainwater, while filled symbols indicate values after removing the rainwater. The value of 6.6 is the Redfield C/N uptake ratio (approximately 106/16; Redfield et al., 1963). The solid line indicates the pCO_2 equilibrium between the seawater and the atmosphere. In **(b)**, the open and semi-filled symbols denote the estimated sea surface pCO_2 from $\Delta DIC–6.6\Delta NO_3$ on top of the mixing with and without rainwater, respectively. The filled symbols denote the field observed sea surface pCO_2, which were obtained by applying TAlk and DIC data into the CO2SYS program (Lewis and Wallace, 1998). The solid line denotes the atmospheric pCO_2 of ~ 390 µatm (Evans et al., 2011).

BGD
11, 7389–7412, 2014